A Coupled Density Functional–Molecular Mechanics Monte Carlo Simulation Method: The Water Molecule in Liquid Water

I. TUÑÓN,[†] M. T. C. MARTINS-COSTA, C. MILLOT, M. F. RUIZ-LÓPEZ,* and J. L. RIVAIL

Laboratoire de Chimie Théorique-UA CNRS 510,[‡] Université Henri Poincaré, Nancy I, B.P. 239, 54506 Vandoeuvre-lès-Nancy Cedex, France

Received 14 November 1994; accepted 20 April 1995

ABSTRACT

A theoretical model to investigate chemical processes in solution is described. It is based on the use of a coupled density functional/molecular mechanics Hamiltonian. The most interesting feature of the method is that it allows a detailed study of the solute's electronic distribution and of its fluctuations. We present the results for isothermal-isobaric constant-NPT Monte Carlo simulation of a water molecule in liquid water. The quantum subsystem is described using a double-zeta quality basis set with polarization orbitals and nonlocal exchange-correlation corrections. The classical system is constituted by 128 classical TIP3P or Simple Point Charge (SPC) water molecules. The atom–atom radial distribution functions present a good agreement with the experimental curves. Differences with respect to the classical simulation are discussed. The instantaneous and the averaged polarization of the quantum molecule are also analyzed.

Introduction

Computer simulation is a powerful tool to study liquid phase phenomena, such as solvation processes or chemical reactions in solution.[1–3] The main limitation of classical simulations is the calibration of the potential used to calculate the interactions between the molecules present in the liquid. Usually, potential functions are developed using the pair approximation, and

*Author to whom all correspondence should be addressed.
[‡]On leave from the Departamento de Química Física, Universidad de Valencia, Valencia, Spain.
[†]Part of the Institut Nancéien de Chimie Moléculaire.

Journal of Computational Chemistry, Vol. 17, No. 1, 19–29 (1996)

CCC 0192-8651 / 96 / 010019-11

therefore they are not able to describe nonadditive effects properly. Although much effort is being expended to overcome this problem (e.g., by the explicit inclusion of many-body terms[4-6], it is difficult to develop potential functions of this type for any general chemical species. Another limitation of the potentials currently employed in computer simulations is that they do not allow a correct description of bond breaking and forming during chemical reactions, spectroscopical properties, or other physical and chemical properties which require a detailed quantum mechanical study.

A full quantum treatment of a liquid or a solution, as it is made in the Car-Parrinello approach,[7,8] overcomes in principle these problems, but because of its cost it is actually limited to medium-size systems. On the other hand, in most of solvation or reactive processes, a reduced number of atoms is directly involved, and it seems reasonable to limit the quantum mechanical treatment to this part. In this way, quantum calculations have been carried out on molecules surrounded by configurations of classical molecules generated from a classical trajectory.[9,10] This type of approach is very useful to get a deeper insight into some averaged properties, but the solute–solvent potential function to be used for the classical simulation can hardly be obtained in some cases. The use of combined quantum mechanical (QM) and molecular mechanics (MM) potentials[11,12] has been proposed as a way to perform coupled simulations. In this approach, the quantum calculations are carried out during the simulation, and energy as well as energy derivatives of the quantum subsystem are used to generate the trajectory. In spite of the great computational effort needed to carry out this kind of simulation, this approach allows the investigation of polarization effects and reactive processes of the quantum part in solution. Moreover, part of the hard work required to develop effective potentials for each new solute is overcome with this technique. Because of computational cost, the quantum part has usually been modeled by a semiempirical Hamiltonian. This QM/MM approach has been implemented both in Monte Carlo[13,14] and molecular dynamics,[15] with promising results. However, quantitative results can hardly be obtained with semiempirical methods, and many systems are not well represented by semiempirical Hamiltonians, so they require a cumbersome reparameterization of the method.

Extension of the QM/MM approach to *ab initio* methods is possible in principle. Nevertheless, the cost would increase quickly with the size of the system, especially because quantitative results usually require taking electron correlation effects into account. As an alternative to semiempirical and *ab initio* approaches, density functional theory (DFT) techniques, which have been remarkably improved in recent years,[16] are promising. They show advantages of generality and often of accuracy with respect to semiempirical methods and of computational speed with respect to correlated traditional *ab initio* methods. Moreover, DFT techniques, with nonlocal corrections to the energy, have been shown to reproduce correctly hydrogen bonds and cooperative effects in solution.[17-19] The development of new correlation-exchange functionals makes possible a systematic improvement of the results found with these methods. To our knowledge, DFT/MM potentials have been implemented recently only in a molecular dynamic program[20] and used to study ions in water, although very little details of the computational method have been given in that work. Here, we present an implementation of the DFT/MM potential in a Monte Carlo NPT simulation. As we shall show, the use of a Monte Carlo technique offers some computational advantages for implementing the DFT/MM potential and allows us to deal with nonlocal corrections in a reasonable amount of computer time. In this article we present the methodology and a first application to the study of a DFT water molecule in a box of classical water molecules. Water has been chosen because experimental information and theoretical results are available and because polarization effects are known to be important in this system.

Methodology

ENERGY CALCULATION

The energy of the whole system is given by the sum of three contributions: the energy of the subsystem described quantum mechanically (*dft*), the energy of the system described at the classical mechanical level (*mm*), and a mixing term (*dft/mm*):

$$E = E_{dft} + E_{mm} + E_{dft/mm} \qquad (1)$$

Both the E_{dft} and the $E_{dft/mm}$ terms depend on the electronic density of the quantum subsystem ($\rho(\mathbf{r}) = \Sigma_i \psi_i(\mathbf{r})\psi_i(\mathbf{r})$) that is obtained by solving

self-consistently the Kohn-Sham equations,[21] in which the solvent electrostatic potential is included:

$$\left[-\frac{\hbar^2}{2m}\nabla^2 - \left(\sum_n \frac{eZ_n}{r_{in}} + \sum_s \frac{eq_s}{r_{is}}\right) + \int d\mathbf{r}' \frac{\rho(\mathbf{r}')}{|\mathbf{r}-\mathbf{r}'|} + \frac{\delta E_{xc}}{\delta\rho(\mathbf{r})}\right]\psi_i(\mathbf{r}) = \varepsilon_i\psi_i(\mathbf{r}) \quad (2)$$

Here, ψ_i is the molecular orbital of electron i, E_{xc} is the exchange-correlation functional, n runs over the nuclei of the quantum system, and s runs over solvent sites.

Once the Kohn-Sham equations are solved, the energy terms can be computed as follows:

$$E_{dft} = -\frac{\hbar^2}{2m}\int d\mathbf{r}\sum_i \psi_i(\mathbf{r})\nabla^2\psi_i(\mathbf{r}) + \int d\mathbf{r}\sum_n \frac{Z_n}{|\mathbf{r}_n-\mathbf{r}|}\rho(\mathbf{r}) + \frac{1}{2}\int\int d\mathbf{r}\,d\mathbf{r}'\frac{\rho(\mathbf{r})\rho(\mathbf{r}')}{|\mathbf{r}-\mathbf{r}'|} + E_{xc}[\rho(\mathbf{r})] + \sum_n\sum_{n'>n}\frac{Z_nZ_{n'}}{r_{nn'}} \quad (3)$$

$$E_{dft/mm} = \int d\mathbf{r}\sum_s \frac{q_s}{|\mathbf{r}_s-\mathbf{r}|}\rho(\mathbf{r}) + \sum_{n,s}\frac{q_sZ_n}{r_{sn}} + \sum_{s,n}V_{sn} \quad (4)$$

The last term of $E_{dft/mm}$ is the crossed van der Waals energy term between quantum nuclei and solvent interaction sites. In the present application, the van der Waals energy is calculated by means of the Lennard-Jones expression

$$V_{ij} = 4\varepsilon_{ij}\left[\left(\frac{\sigma_{ij}}{r_{ij}}\right)^{12} - \left(\frac{\sigma_{ij}}{r_{ij}}\right)^{6}\right] \quad (5)$$

The molecular mechanics energy term is given by the classical equation

$$E_{mm} = \sum_{s,s'}\frac{q_sq_{s'}}{r_{ss'}} + \sum_{s,s'}V_{ss'} \quad (6)$$

where s and s' run over solvent sites of different molecules and $V_{ss'}$ is computed using eq. (5).

COMPUTATIONAL STRATEGIES

The practical implementation of the DFT/MM potential in an NPT Monte Carlo simulation has been done as follows: A new configuration is generated by moving one classical molecule chosen at random. After a given number of steps, the position of the quantum molecule or the volume is also randomly changed. For each new configuration, the total energy [eq. (1)] is computed to carry out the Metropolis test. If the configuration is accepted, the averaged quantitites are updated and the new wave function is stored to be used at the next step as the SCF initial guess.

In principle, the computation of the total energy at each step of the simulation requires the solution of the Kohn-Sham equations for the current configuration. However, to save computer time, we can take advantage of the nature of the Monte Carlo algorithm. In contrast with molecular dynamics simulations, only one molecule is displaced in most of the Monte Carlo moves. Thus, we have employed a simple criterion to decide when to carry out a self-consistent DFT calculation. It is performed when the solute moves, the volume changes, or the displaced solvent molecule lies in or enters at least one of the spheres of radius r_d centered on the quantum atoms. When the distance of the center of mass of the displaced solvent molecule to each atom of the quantum system is larger than r_d, a frozen electronic density approximation is made. In this case, the total *dft/mm* energy at the j-step is effectively calculated as

$$E^j_{dft/mm} = E^{j-1}_{dft/mm} + \sum_s q_s\left[\int d\mathbf{r}\frac{\rho^{j-1}(\mathbf{r})}{|\mathbf{r}^j_s-\mathbf{r}|} - \int d\mathbf{r}\frac{\rho^{j-1}(\mathbf{r})}{|\mathbf{r}^{j-1}_s-\mathbf{r}|}\right] + \sum_{s,n}\left[\frac{q_sZ_n}{r^j_{sn}} - \frac{q_sZ_n}{r^{j-1}_{sn}}\right] + \sum_{s,n}\left[V^j_{s,n} - V^{j-1}_{s,n}\right] \quad (7)$$

where $\rho^{j-1}(\mathbf{r})$ is the electronic density of the quantum part in the last accepted configuration and the sum over s runs only for the charges of the displaced solvent molecule. Therefore, this approach leads to an efficient computation of the energy since only the integrals for the charges of the displaced solvent molecule need to be recomputed. The r_d distance can be selected by comparing the energy computed in the frozen density approach and in the self-consistent DFT calculation. From some test calculations using simple solute–solvent systems, we empirically found that an r_d value including the two first solvation shells

was a good compromise. This substantially reduces the number of self-consistent DFT calculations required, which represents typically 25 to 40% of the total number of steps in a simulation. To illustrate this point, we present some results for a case expected to be highly sensitive to polarization effects: the DFT chloride anion in the presence of a positive unit charge. Two kinds of calculations have been carried out. First, SCF computations for the chlorine ion interacting with a positive charge were performed.[§] Second, the electrostatic energy corresponding to the interaction of the positive charge and the chlorine ion with a frozen density was evaluated. Comparison of both results is made in Figure 1 for different values of the chlorine anion–positive charge distances. The energy difference decreases very fast with increasing distance, so for distances larger than 5 Å it is smaller than -0.3 kcal mol^{-1}. This may be considered an upper limit of the error due to the frozen-density approximation, which has been shown to be much smaller in test simulations of liquid water that we have carried out. Thus, the average quantum water molecule–classic solvent water molecules interaction energy obtained in a Monte Carlo simulation of 10,000 steps is essentially the same ($\delta < 0.01$ kcal mol^{-1}) when the computation is carried out using the frozen-density approach for distances larger than $r_d = 5.0$ Å or when it is performed without this approximation. This roughly means that only movements that imply changes in the first and second solvation shell need to be treated at the self-consistent DFT level.

[§]Calculations carried out with the (6321/521/1*) basis sets for the chlorine anion and employing Becke-Perdew nonlocal corrections (see refs. 25–27).

Another interesting aspect of the implementation of the DFT/MM potential in a Monte Carlo simulation is the treatment of nonlocal exchange-correlation energy contributions. These terms are important in the study of molecular interactions, such as hydrogen bonding,[17–19] and their inclusion can be decisive for a correct reproduction of liquid properties. Since energy only is needed in a Monte Carlo procedure, the Kohn-Sham equations can be solved at the local level and nonlocal corrections to the energy introduced after the iterative process. Figure 2 shows the potential energy curves for a model system (fluorine anion–water molecule) calculated using the mixed procedure and the self-consistent treatment of nonlocal corrections.[‖] The curves exhibit parallel evolutions, especially in the attractive part. This means that the interaction energies predicted should not depend much on the method used to treat nonlocal corrections. Hence, the post-SCF approximation is convenient for Monte Carlo simulations, either to generate new configurations or to compute solvation enthalpies. In the case of the fluorine anion–water molecule, this mixed procedure reduces the computation time by a factor of 2 compared with the self-consistent treatment of nonlocal corrections.

COMPUTATIONAL DETAILS

Monte Carlo simulations have been performed in a cubic box of 15.6 Å of side with 128 TIP3P (ref. 22) water molecules and a DFT water molecule at 25°C and 1 atm using the NPT ensemble.[23] Periodic boundary conditions and a cutoff distance of

[‖]Calculations carried out using the basis set F(621/41/1*), O(621/41/1*), H(41), and Perdew nonlocal corrections for exchange and correlation (see refs. 25–27).

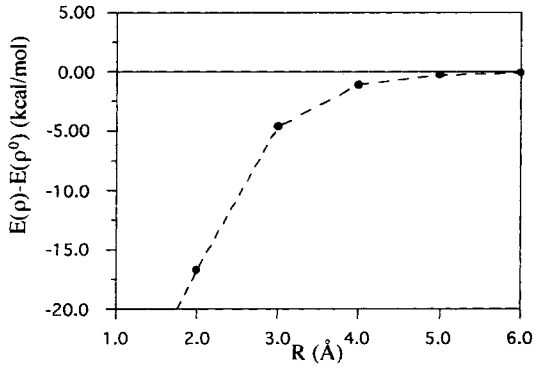

FIGURE 1. Energy difference between the frozen density and self-consistent DFT calculations for the chlorine anion-unit positive charge system as function of the distance.

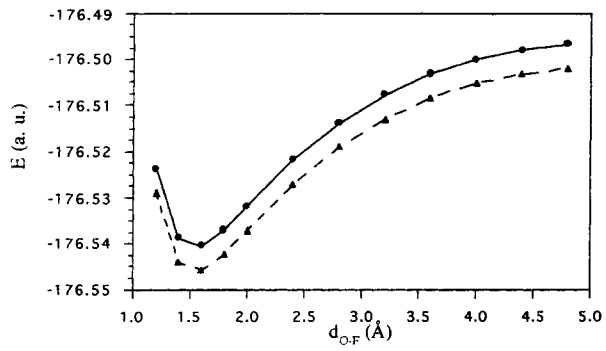

FIGURE 2. DFT energy curves for the fluorine anion–water molecule system calculated incorporating nonlocal corrections self-consistently (filled triangles) or after resolution of the Kohn-Sham equations (filled circles).

7.6 Å have been applied for all classical–classical and classical–quantic interactions. Metropolis sampling has been supplemented by preferential sampling[24] with $1/(r^2 + c)$ weighting, where $c = 150$ Å^2. Solute displacements and volume changes have been attempted every 75 and 1250 steps, respectively. The new configurations have been thus generated moving the solute or the solvent molecules randomly in the three Cartesian directions and changing randomly the quaternions that define the orientation. When the volume is changed, the positions of all the molecules are conveniently rescaled. The ranges of these motions have been chosen to provide an acceptance ratio of ca. 45% for the new configurations. Equilibration was carried out during 2.0 M configurations followed by averaging over 3.0 M configurations.

The geometry and the Lennard-Jones parameters of the DFT water molecule were those of the TIP3P water monomer ($d = 0.9572$ Å, $\alpha = 104.52°$). Kohn-Sham equations were self-consistently solved at the local level with the Vosko-Wilk-Nusair (VWN) potential[25] using the deMon program,[26] which has been modified to include the solvent point charge potential. The basis sets used were H(41) and O(621/41/1).[26] Auxiliary basis sets used in the fitting of the charge density and the exchange-correlation potential were H(4;4) and O(4,3;4,3).[26] After the iterative procedure, nonlocal corrections were added using the density gradient corrections proposed by Becke for the exchange and Perdew for the correlation term.[27,28] Numerical integration of the exchange-correlation contribution is computed on a MEDIUM grid.[26] The r_d distance used to define the frozen density approach was 5.0 Å both for oxygen and hydrogen atoms of the quantum molecule. This value is slightly greater than the oxygen–oxygen distance corresponding to the second solvation shell peak in the experimental radial distribution function. As noted earlier, test simulations have shown that this is a very good approximation and that increasing the value of r_d is not expected to modify the results of the simulation. An additional condition has been imposed to assure that no more than 10 steps can be carried out without updating the electronic density. This provides about 25% of self-consistent DFT calculations during the simulation. Although the inclusion of polarization functions and nonlocal corrections considerably increases the computational time needed to carry out the simulation, we think that they are important to check the real performance of the DFT/MM potential. Moreover, these calculations should be useful as a test for future simplified treatments, such as the use of smaller basis sets of pseudopotentials, or modifications of the algorithm to reduce the frequency of self-consistent DFT calculations.

Results and Discussion

DFT/MM POTENTIAL TESTS

Computations on the water dimer have been carried out to test the DFT/MM potential described earlier. Results are presented in Table I for the quantum dimer, the quantum acceptor–classical donor dimer, and the quantum donor–classical acceptor dimer. Geometrical parameters refer to Figure 3. Calculations at the DFT and DFT/MM levels have been carried out using the same basis sets and include nonlocal corrections. DFT calculations have been carried out with full geometry optimization. Minimization of the DFT/TIP3P dimers has been carried out using a gradient method, keeping the internal geometry of the monomers fixed to the TIP3P values. At the DFT level, the water dimer is properly described, although the oxygen–oxygen distance is a little shorter than the experimental[29] and *ab initio* distances.[30] The association energy is underestimated by 1.1 kcal mol^{-1}. Similar tendencies for the water dimer have been obtained using more extended basis sets.[31,32]

Using the DFT/TIP3P potential, we have located two minima, with the quantum molecule acting as proton acceptor or as proton donor. In both cases, the oxygen–oxygen distances are shorter than the experimental one (0.2 Å and 0.3 Å, respectively) and the association energies are overestimated. Note that using the TIP3P potential, similar deviations with respect to the experimental geometry are obtained.[22] Our potential preserves

TABLE I.
Models of Water Dimer.

Dimer	d(0102)	α	β	ΔE
Exp[a]	2.98	57.0	−1.0	−5.4
DFT[b]	2.87	58.7	1.7	−4.3
DFT/MM				
Quantum acceptor	2.77	61.3	0.6	−6.8
Quantum donor	2.68	16.0	−1.0	−7.7

Geometry refers to Figure 3. Distances are given in angstroms, angles in degrees, and energies in kcal/mol.
[a] Ref. 29.
[b] See text.

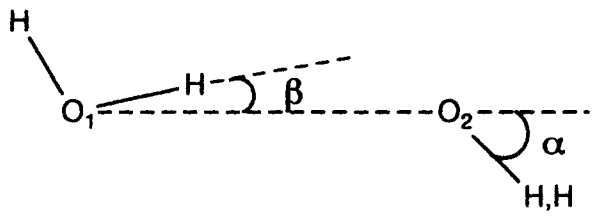

FIGURE 3. Geometry of the water dimer.

the C_s symmetry and correctly describes the relative orientation of the dimer, in particular when the quantum molecule acts as the proton acceptor molecule, wherein the agreement with experiment is very good. These results show that our DFT/TIP3P potential gives a reasonable description of the water dimer. An improved DFT/MM potential could be developed in principle. The simplest modification would concern the Lennard-Jones term of the quantum molecule in order to adapt it to the quantum molecule electrostatic properties. We are presently investigating this possibility.

RADIAL DISTRIBUTION FUNCTIONS

Let us consider the radial distribution functions (RDF) obtained by averaging the quantum water molecule–solvent molecule distances. Table II presents the results obtained for the RDF main peak positions compared to experimental data[33] and to classical TIP3P simulation results. The RDF for oxygen–oxygen, oxygen–hydrogen, and hydrogen–hydrogen are plotted in Figures 4, 5, and 6, respectively. For comparison, the oxygen–oxygen RDF obtained from an AM1/TIP3P simulation is also provided in Figure 4a. This RDF is poorly structured and clearly shows the failure of the AM1 semiempirical method to deal with some hydrogen-bonded systems and the need to develop more accurate QM/MM potentials. The DFT/TIP3P oxygen–oxygen RDF has the correct structure, with two peaks clearly differentiated. The first oxygen–oxygen peak appears at a distance shorter than the experimental value (2.72 Å versus 2.88 Å). The first minimum also appears at a shorter distance (3.28 Å versus 3.34 Å) and is deeper than the experimental one, reflecting the overestimation of the interaction energies obtained for the dimer. However, the coordination number obtained from integration of the calculated quantum oxygen–classical oxygen curve nearly matches that obtained from the experimental RDF (4.2 and 4.4, respectively). The second peak appears at larger oxygen–oxygen distances than the experimental one. Since the influence of the classical model is much more important for this second peak, we have decided to carry out a second simulation changing the classical solvent model. An NPT Monte Carlo simulation has been performed by using the SPC[34] model of water, which is known to reproduce the second peak of the oxygen–oxygen RDF better than the TIP3P model. The results obtained after 2 M Monte Carlo steps are presented in Figure 4b. The first peak of the DFT/SPC oxygen–oxygen radial distribution function is placed at the same position as the DFT/TIP3P curve, although the former is slightly more intense than the latter. The second peak of the DFT/SPC seems to be in better agreement with the experimental RDF than the DFT/TIP3P peak, although the noise level precludes a definitive conclusion.

The oxygen–hydrogen RDFs are given in Figure 5. We have obtained two different curves: that corresponding to the quantum oxygen–classic hydrogen and that of quantum hydrogen–classic oxygen. As expected from the analysis of the water dimer, the quantum hydrogen–classical oxygen

TABLE II.
Experimental and Calculated Properties of Water.

	Exp.	TIP3P	DFT / TIP3P
RDF first peak			
O—O	2.88[a]	2.76	2.72
O—H	1.85[a]	1.82	1.80[b]
			1.75[c]
H—H	2.33[a]	2.45	2.38
RDF second peak			
O—O	4.50[a]	—	4.92
O—H	3.27[a]	3.21	3.23[b]
			3.13[c]
H—H	3.84[a]	3.77	3.74
Dipole moment			
μ_g	1.85[d]	2.35	2.28
μ_s	2.6[e]	2.35	2.89(±0.04)[f]
$\Delta\mu$	0.75	—	0.61(±0.05)[f]
ΔH_{sol}	−10.5[g]	−10.4[h]	−13.2(±2)[f]

Positions of peaks in Å, dipole moments in debye, and solvation enthalpies in kcal / mol.
[a]Ref. 33.
[b]Quantum oxygen–classical hydrogen.
[c]Quantum hydrogen–classical oxygen.
[d]Ref. 35.
[e]In ice, refs. 37 and 38.
[f]Number in parentheses is the standard deviation.
[g]Ref. 36.
[h]Ref. 22.

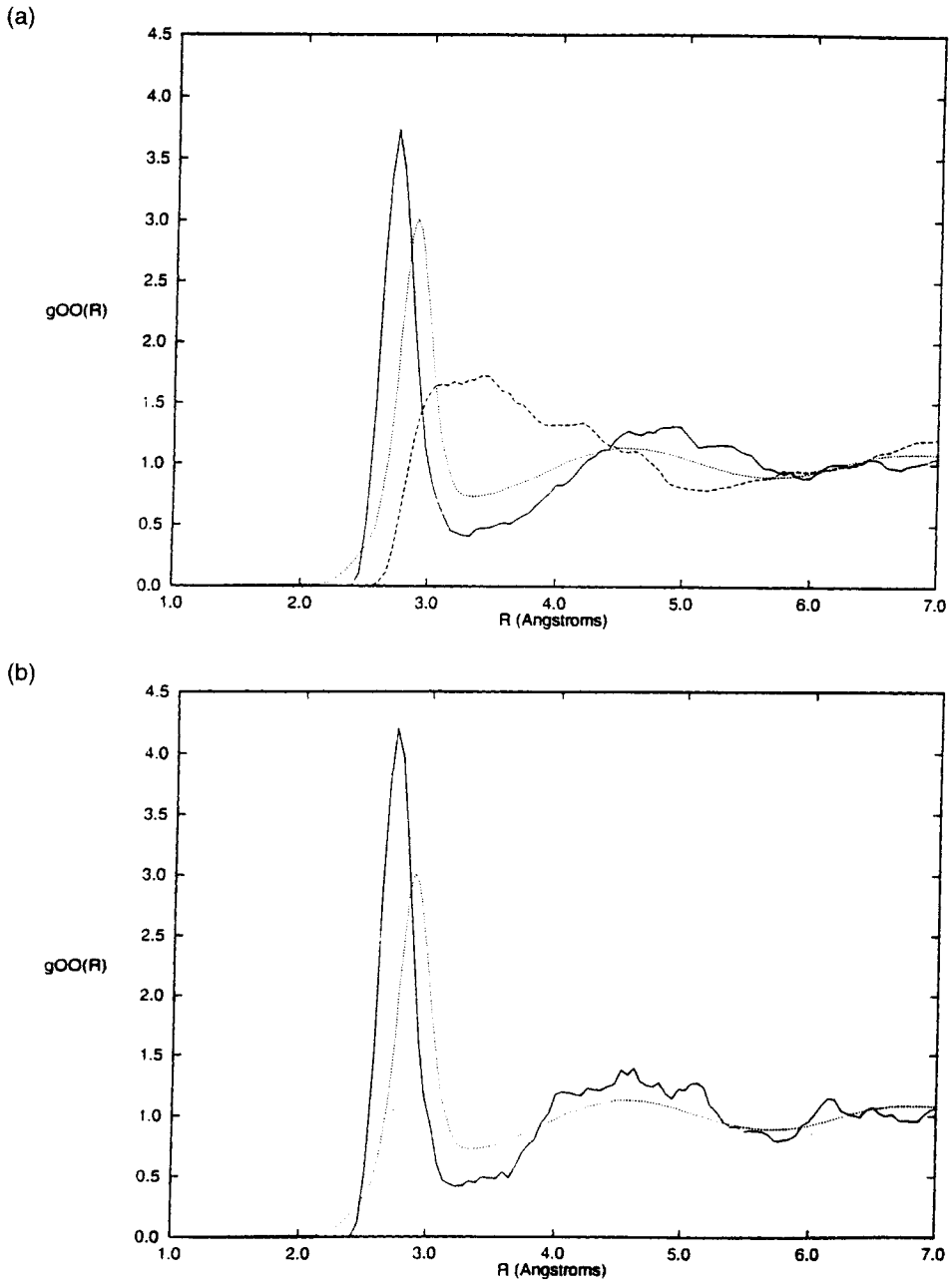

FIGURE 4. Oxygen–oxygen radial distribution functions. (a) DFT / TIP3P (normal line), AM1 / TIP3P (dashed line), and experimental (dotted line). (b) DFT / SPC (normal line) and experimental (dotted line).

RDF appears at slightly shorter distances than the quantum oxygen–classical hydrogen RDF, and the intensity of the peaks is also slightly larger because of the more negative association energy of the dimer when the quantum water molecule acts as proton donor. In comparison with the experimental RDF, both calculated curves are displaced to the left and present an overestimated first peak. The minima are also deeper than the experimental one, as was found for the oxygen–oxygen RDF.

The hydrogen–hydrogen RDFs are given in Figure 6. The DFT/TIP3P RDF presents two well-located peaks with respect to the experimental curve, although the intensity of the first one is also larger. The correct position of the peaks could be a consequence of error cancellation between dis-

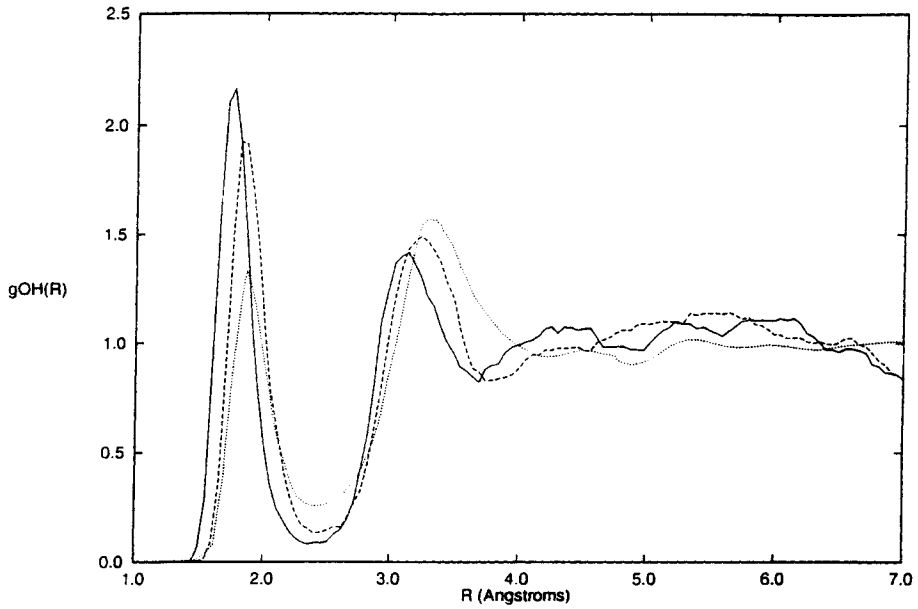

FIGURE 5. Oxygen–hydrogen radial distribution functions: DFT hydrogen–TIP3P oxygen (normal line), DFT oxygen–TIP3P hydrogen (dashed line), and experimental (dotted line).

tances and orientation (see dimer results). Again, the first minimum is slightly deeper than the experimental one.

SOLUTE POLARIZATION

Let us analyze the polarization of the quantum water molecule. The calculated dipole moments in gas phase and in solution are given in Table II. The calculated gas-phase dipole moment is substantially overestimated. This is not surprising since we use in this exploratory work a rather limited basis set, and it has been previously shown[9] that large basis sets are needed to reproduce correctly the experimental dipole moment. For instance, using a triple-zeta quality basis set including diffuse

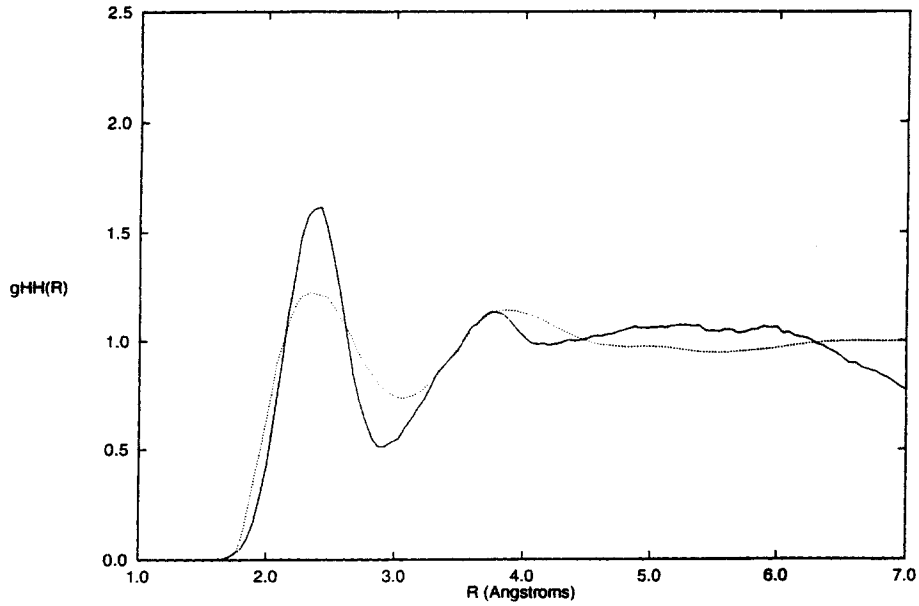

FIGURE 6. Hydrogen–hydrogen radial distribution functions: DFT / TIP3P (normal line) and experimental (dotted line).

functions, Salahub et al. obtained a dipole moment in the gas phase of 1.81 debye[9] which is very close to the experimental value.[35] When the quantum water molecule is placed into the classical liquid, the electronic distribution is substantially polarized. The averaged dipole moment obtained at the end of the simulation (2.89 debye) is very close to that obtained in a recent simulation using an anisotropic polarizable water model (2.81 debye),[36] but it is again substantially larger than the experimental estimate for ice (about 2.6 debye)[37,38] and than the result of a Car-Parrinello simulation of liquid water (2.66 debye).[8] The averaged induced dipole moment, obtained from the difference between the values in vacuo and in solution, is 0.61 debye. This value is in fairly good agreement with the experimental induced dipole moment from the gas phase to ice (0.75 debye). One can expect to improve this agreement by using a larger basis set, in particular by including diffuse functions, since the water polarizability would be larger. Note, however, that the induced moment also depends on the radial distribution functions, which are, in turn, dependent on the potential employed to generate the configurations. At this point, it is interesting to compare our results with those obtained by Salahub et al.[9] using the same basis set and a selected number of configurations chosen from a classical TIP3P simulation of liquid water. These authors obtained an induced dipole moment of 0.41 debye.[9] The difference between this value and ours (0.20 debye) is essentially due to the relaxation of the classical solvent in the presence of the quantum molecule. In fact, this has a non-negligible influence on the RDFs, as shown in Table II, and consequently on the polarization of the quantum subsystem.

Finally, our results show that changes in the electronic density of the quantum molecule due to modifications of the liquid environment may be considerably large. Figure 7 presents the averaged and instantaneous dipole moment of the DFT moelcule along 1.5-M configurations of the simulation. The dipole moment oscillates between 2.70 and 3.10 debye, about 14% of the total dipole moment. These fluctuations of the electronic density induced by the solvent may play a decisive role in the reactivity of some chemical species in solution.

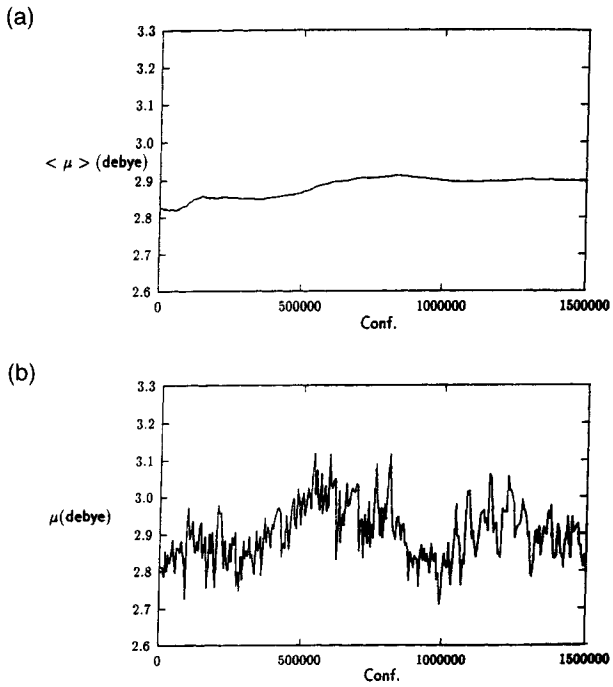

FIGURE 7. Cumulative average (a) and instantaneous value (b) of the DFT water molecule dipole moment along 1.5-M step run.

ENERGETICS

The solvation enthalpy of the quantum molecule (see Table II) has been calculated as

$$\Delta H_{sol} = \Delta H_{sim} - \Delta H_{liq} - E_{gas} - RT$$

where ΔH_{sim} is the total enthalpy of the simulation, ΔH_{liq} is the enthalpy of 128 TIP3P water molecules, and E_{gas} is the DFT energy of the water molecule in vacuo. The calculated solvation enthalpy is somewhat larger than the experimental value,[39] as could be expected from the results obtained for the DFT/TIP3P water dimer association energies. The obtained intermolecular energy is -12.6 kcal/mol, while the experimental estimate (see ref. 22) is -9.9 kcal/mol. In quantum calculations using classical TIP3P simulations, Salahub et al.[9] estimated intermolecular energies slightly smaller (-10.4 kcal/mol). The difference between this result and that of our simulation (2.2 kcal/mol) can be mainly attributed to the relaxation of the classical solvent in the presence of the quantum molecule. The introduction of this degree of freedom leads to a stabilization of the system and consequently to larger interaction energies.

Conclusions

In this article we have presented a method to study solution processes through the use of a cou-

pled DFT/MM potential. Simulations for the water molecule in liquid water have been carried out implementing the DFT/TIP3P potential in an NPT Monte Carlo program. The results regarding energy, polarization effects, and radial distribution functions are satisfactory, taking into account the fact that the Lennard-Jones term of the quantum molecule has not been reoptimized for this specific application. The study of the quantum-classical water dimer shows that this term can be modified to improve the equilibrium intermolecular distances.

The potential used gives acceptable radial distribution functions with two well-defined peaks. In general, the peaks appear at distances shorter than the experimental RDF and the first minima are slightly deeper, corresponding to an interaction energy larger than the experimental one. The change of the classical solvent model from TIP3P to SPC does not modify the position of the first peak of the oxygen–oxygen RDF, but it seems to have an important effect on the second one, leading to a better agreement with experiment.

The use of coupled quantum mechanics/molecular mechanics potential allows the study of physical properties of the quantum subsystems, such as solute polarization in solution. In the present study, with a double-zeta quality basis set and polarization functions on the oxygen atom, we have obtained an averaged induced dipole moment of 0.61 debye, resulting in a final dipole moment in solution of 2.89 debye.

Comparison of our results with those obtained by Salahub et al.[9] from DFT calculations on a selected number of solvent configurations obtained from a classical simulation of liquid water shows that the solvent relaxation under the influence of the quantum molecule has non-negligible effects both on the polarization and on the interaction energies. Moreover, it has been shown that variations of the instantaneous dipole moment of the quantum water molecule are as large as 0.4 debye. These fluctuations are expected to play an important role in reactive processes. Hence, the use of coupled DFT/MM potentials appears to be a useful tool to investigate chemical processes in solution by using Monte Carlo or molecular dynamics techniques.

Acknowledgments

I. T. acknowledges the warm hospitality of all the members of the Laboratoire de Chimie Théorique and a postdoctoral fellowship of the Ministerio de Educación y Ciencia (Spain).

References

1. M. P. Allen and D. J. Tildesley, *Computer Simulation of Liquids*, Oxford University Press, New York, p. 212, 1987.
2. J. Chandrasekhar, S. F. Smith, and W. L. Jorgensen, *J. Am. Chem. Soc.*, **107**, 154 (1985).
3. P. Kollman, *Chem. Rev.*, **93**, 2395 (1993).
4. M. Sprik, M. L. Klein, and K. Watanabe, *J. Phys. Chem.*, **94**, 6483 (1990).
5. L. X. Dang, J. E. Rice, J. Caldwell, and P. A. Kollman, *J. Am. Chem. Soc.*, **113**, 2481 (1991).
6. C. Millot and A. J. Stone, *Molec. Phys.*, **77**, 439 (1992).
7. R. Car and P. Parrinello, *Phys. Rev. Lett.*, **22**, 2471 (1985).
8. K. Laasonen, M. Sprik, M. Parrinello, and R. Car, *J. Chem. Phys.*, **99**, 9089 (1993).
9. D. Wei and D. R. Salahub, *Chem. Phys. Lett.*, **224**, 291 (1994).
10. (a) G. Jansen, J. G. Àngyàn, and F. Colonna, *Proceedings of the First European Conference on Computational Chemistry*, F. Bernardi, Ed., American Institute of Physics (in press); (b) G. Jansen, F. Colonna, and J. G. Àngyàn, *Int. J. Quantum Chem.*, in press.
11. (a) A. Warshel and M. Levitt, *J. Mol. Biol.*, **103**, 227 (1976); (b) A. Warshel, *J. Phys. Chem.*, **83**, 1640 (1979); (c) V. Luzhkov and A. Warshel, *J. Comp. Chem.*, **13**, 199 (1992).
12. M. J. Field, P. A. Bash, and M. Karplus, *J. Comp. Chem.*, **11**, 700 (1990).
13. J. Gao and X. Xia, *Science*, **258**, 631 (1992).
14. J. Gao, *J. Phys. Chem.*, **96**, 537 (1992).
15. P. Bash, M. J. Field, and M. Karplus, *J. Am. Chem. Soc.*, **109**, 8092 (1987).
16. R. G. Parr and W. Yang, *Density-Functional Theory of Atoms and Molecules*, Oxford University Press, New York, 1989.
17. M. F. Ruiz-López, F. Bohr, M. T. C. Martins-Costa, and D. Rinaldi, *Chem. Phys. Lett.*, **221**, 109 (1994).
18. F. Sim, A. St-Amant, I. Papai, and D. R. Salahub, *J. Am. Chem. Soc.*, **114**, 4391 (1992).
19. C. Mijoule, Z. Latajka, and D. Borgis, *Chem. Phys. Lett.*, **208**, 364 (1993).
20. R. V. Stanton, D. V. Hartsough, and K. N. Merz, Jr., *J. Phys. Chem.*, **97**, 11868 (1993).
21. W. Kohn and L. J. Sham, Phys. Rev. A, **140**, 1133 (1965).
22. W. L. Jorgensen, J. Chandrashekar, J. Madura, R. W. Impey, and M. L. Klein, *J. Chem. Phys.*, **79**, 926 (1983).
23. (a) W. W. Wood, In *Physics of Simple Liquids*, H. N. V. Temperley, J. S. Rowlinson, and G. S. Rushbrooke, Eds., North-Holland, Amsterdam, 1968, p. 115; (b) W. W. Wood, *J. Chem. Phys.*, **48**, 415 (1968); (c) W. W. Wood, *J. Chem. Phys.*, **52**, 729 (1970).
24. J. C. Owicki, *ACS Symp. Ser.*, **86**, 159 (1978).
25. S. H. Vosko, L. Wilk, and M. Nusair, *Can. J. Phys.*, **58**, 1200 (1980).
26. (a) A St-Amant and D. R. Salahub, *Chem. Phys. Lett.*, **169**, 387 (1990); (b) D. R. Salahub, R. Fournier, P. Mlynarski, I. Papai, A. St-Amant, and J. Ushio, In *Theory and Applications of Density Functional Approaches to Chemistry*, J. Labanowski and J. Andzelm, Eds., Springer-Verlag, Berlin, p. 77, 1991.

27. A. D. Becke, *Phys. Rev. A*, **38**, 3098 (1988).
28. (a) J. P. Perdew, *Phys. Rev. B*, **38**, 8822 (1986); (b) Ibid., **34**, 7406 (1986).
29. L. A. Curtiss, D. J. Frurip, and M. Blander, *J. Chem. Phys.*, **71**, 2703 (1979).
30. J. Bertrán, M. F. Ruiz-López, D. Rinaldi, and J. L. Rivail, *Theor. Chim. Acta*, **84**, 181 (1992).
31. Y. Jeanvoine, F. Bohr, and M. F. Ruiz-Lopez, *Can. J. Chem.*, **73**, 710 (1995).
32. F. Sim, A. St-Amant, I. Papai, and D. R. Salahub, *J. Am. Chem. Soc.*, **114**, 4391 (1992).
33. A. K. Soper and M. G. Phillips, *Chem. Phys.*, **67**, 47 (1986).
34. H. J. C. Berendsen, J. P. M. Postma, W. F. van Gunsteren, and H. J. Hermans, In *Intermolecular Forces*, B. Pullman, Ed., Reidel, Dordrecht, 1981, p. 331.
35. S. A. Clough, Y. Beers, G. P. Klein, and L. S. Rothman, *J. Chem. Phys.*, **59**, 2254 (1973).
36. D. N. Bernardo, Y. Ding, K. Krogh-Jespersen, and R. M. Levy, *J. Phys. Chem.*, **98**, 4180 (1994).
37. C. A. Coulson and D. Eisenberg, *Proc. Roy. Soc. London A*, **291**, 445 (1966).
38. E. Whalley, *Chem. Phys. Lett.*, **53**, 449 (1978).
39. G. S. Kell, *J. Chem. Eng. Data*, **20**, 97 (1975).